

Wrong sign Yukawa coupling of 2HDM with a scalar dark matter confronted with dark matter and Higgs data

Lei Wang, Rongle Shi, Xiao-Fang Han

Department of Physics, Yantai University, Yantai 264005, China

Abstract

In the framework of type-II two-Higgs-doublet model with a scalar dark matter (S), we examine the wrong sign Yukawa coupling of the 125 GeV Higgs which is the only portal between dark matter and SM sectors. After imposing the constraints from the Higgs searches at the LHC and dark matter experiments, we obtain some interesting observables: (i) In the case of the wrong sign Yukawa coupling of the 125 GeV Higgs, $\tan\beta$ can be imposed stringent constraints by the theory, oblique parameters and the Higgs searches at the LHC. For example, for $m_H = 600$ GeV and $140 \text{ GeV} < m_A < 200 \text{ GeV}$, $\tan\beta$ is required to be in the range of 4.2 and 5.7. (ii) Due to the contribution of $SS \rightarrow AA$ annihilation channel to the relic density, the dark matter coupling with the 125 GeV Higgs can be sizably suppressed. However, the $SS \rightarrow AA$ channel can not solve the tension between the relic density and the signal data of 125 GeV Higgs for $m_S < 50 \text{ GeV}$. (iii) The limits of XENON1T (2017) and PandaX-II (2017) exclude most of samples in the ranges of $64 \text{ GeV} < m_S < 80 \text{ GeV}$, $0.65 < f^n/f^p < 1$, and $y_d/y_u > -0.91$. Some samples in the ranges of $80 \text{ GeV} < m_S < 116 \text{ GeV}$ and $y_d/y_u > -0.75$ are also excluded by the constraints of XENON1T (2017) and PandaX-II (2017). (iv) The Fermi-LAT limits exclude most of samples in the range of $62.5 \text{ GeV} < m_S < 65 \text{ GeV}$, including the samples with $f^n/f^p \sim -0.7$.

PACS numbers: 12.60.Fr, 14.80.Ec, 14.80.Bn

I. INTRODUCTION

The two-Higgs-doublet model (2HDM) [1] is a simple extension of SM by adding a second $SU(2)_L$ Higgs doublet, which includes two neutral CP-even Higgs bosons h and H , one neutral pseudoscalar A , and two charged Higgs H^\pm in the scalar sector. According to different Yukawa couplings, there are four types of 2HDMs without the tree-level flavor changing neutral currents, type-I [2, 3], type-II [2, 4], lepton-specific, and flipped models [5–8].

In the 2HDM, the 125 GeV Higgs is allowed to have the SM-like coupling and the wrong sign Yukawa coupling. For the former, the tree-level couplings of the 125 GeV Higgs and the SM particles are very close to the SM couplings. For the latter, compared to the SM, at least one of the Yukawa couplings of the 125 GeV Higgs has an opposite sign to the coupling of gauge boson [9–19]. The wrong sign Yukawa coupling of the 125 GeV Higgs is a characteristic of 2HDM, which has some interesting applications. For example, in the lepton-specific model the muon g -2 anomaly can be explained by a light pseudoscalar with a very large $\tan\beta$, and the corresponding 125 GeV Higgs is favored to have the wrong sign Yukawa coupling of lepton [20, 21]. Besides, in the type-II 2HDM with a scalar dark matter (DM), a large isospin-violating DM-nucleon can be realized when the mediator is the 125 GeV Higgs with the wrong sign Yukawa coupling of down-type quark [22–28]. With the rapidly improved sensitivity of DM direct detection experiments, such as LUX (2016) [29], XENON1T (2017) [30] and PandaX-II (2017) [31], the cross section of DM-nucleon has been imposed stringent constraints. The isospin-violating coupling of DM-nucleon can weaken the experimental upper limits on the spin-independent DM-nucleon cross section, especially that f^n/f^p is close to -1, -0.8 and -0.7 for target nucleons Si, Ge and Xe. In addition, the annihilation channels of DM are given strong limits by the Fermi-LAT search for DM annihilation from dwarf spheroidal satellite galaxies (dSphs) [32]. A great deal of ATLAS and CMS searches for scalars at the LHC can impose the strong constraints on the parameter space of type-II 2HDM in the case of the wrong sign Yukawa coupling of the 125 GeV Higgs. In this paper we will examine the wrong sign Yukawa coupling of the 125 GeV Higgs in the type-II 2HDM with a scalar DM considering the joint constraints from the theory, precision electroweak data, flavor observables, the 125 GeV Higgs signal data, and the searches for the additional Higgs at the LHC as well as DM experiments.

Our work is organized as follows. In Sec. II we recapitulate the type-II 2HDM with a scalar DM. In Sec. III we perform numerical calculations. In Sec. IV, we discuss the allowed parameter space after imposing the relevant theoretical and experimental constraints. Finally, we give our conclusion in Sec. V.

II. TYPE-II TWO-HIGGS-DOUBLET MODEL WITH A SCALAR DARK MATTER

A. Type-II two-Higgs-doublet model

The scalar potential with a softly broken discrete Z_2 symmetry is given by [33]

$$\begin{aligned} V = & m_{11}^2(\Phi_1^\dagger\Phi_1) + m_{22}^2(\Phi_2^\dagger\Phi_2) - \left[m_{12}^2(\Phi_1^\dagger\Phi_2 + \text{h.c.}) \right] \\ & + \frac{\lambda_1}{2}(\Phi_1^\dagger\Phi_1)^2 + \frac{\lambda_2}{2}(\Phi_2^\dagger\Phi_2)^2 + \lambda_3(\Phi_1^\dagger\Phi_1)(\Phi_2^\dagger\Phi_2) + \lambda_4(\Phi_1^\dagger\Phi_2)(\Phi_2^\dagger\Phi_1) \\ & + \left[\frac{\lambda_5}{2}(\Phi_1^\dagger\Phi_2)^2 + \text{h.c.} \right]. \end{aligned} \quad (1)$$

We consider the case of the CP-conserving in which all λ_i and m_{12}^2 are real. The two complex Higgs doublets have hypercharge $Y = 1$,

$$\Phi_1 = \begin{pmatrix} \phi_1^+ \\ \frac{1}{\sqrt{2}}(v_1 + \phi_1^0 + ia_1) \end{pmatrix}, \quad \Phi_2 = \begin{pmatrix} \phi_2^+ \\ \frac{1}{\sqrt{2}}(v_2 + \phi_2^0 + ia_2) \end{pmatrix}. \quad (2)$$

Where v_1 and v_2 are the electroweak vacuum expectation values (VEVs) with $v^2 = v_1^2 + v_2^2 = (246 \text{ GeV})^2$. The ratio of the two VEVs is usually defined as $\tan\beta = v_2/v_1$. There are five physical states after spontaneous electroweak symmetry breaking: two neutral CP-even h and H , one neutral pseudoscalar A , and two charged scalars H^\pm .

The Yukawa interactions of type-II 2HDM are given by

$$-\mathcal{L} = Y_{u2} \overline{Q}_L \tilde{\Phi}_2 u_R + Y_{d1} \overline{Q}_L \Phi_1 d_R + Y_{\ell 1} \overline{L}_L \Phi_1 e_R + \text{h.c.}, \quad (3)$$

where $Q_L^T = (u_L, d_L)$, $L_L^T = (\nu_L, l_L)$, $\tilde{\Phi}_{1,2} = i\tau_2 \Phi_{1,2}^*$, and Y_{u2} , Y_{d1} and $Y_{\ell 1}$ are 3×3 matrices in family space.

The Yukawa couplings of the neutral Higgs bosons with respect to the SM are given by

$$\begin{aligned}
y_V^h &= \sin(\beta - \alpha), & y_f^h &= [\sin(\beta - \alpha) + \cos(\beta - \alpha)\kappa_f], \\
y_V^H &= \cos(\beta - \alpha), & y_f^H &= [\cos(\beta - \alpha) - \sin(\beta - \alpha)\kappa_f], \\
y_V^A &= 0, & y_f^A &= -i\kappa_f \text{ (for u)}, & y_f^A &= i\kappa_f \text{ (for d, } \ell), \\
&& \text{with } \kappa_d = \kappa_\ell \equiv -\tan\beta, & \kappa_u \equiv 1/\tan\beta,
\end{aligned} \tag{4}$$

where V denotes Z or W .

In the case of the wrong sign Yukawa coupling, at least one of the Yukawa couplings of the 125 GeV Higgs has the opposite sign to the coupling of gauge boson. However, the 125 GeV Higgs signal data require the absolute values of the Higgs couplings to be close to the SM. Therefore, we can obtain

$$\begin{aligned}
y_h^{fi} &= -1 + \epsilon, & y_h^V &\simeq 1 - 0.5 \cos^2(\beta - \alpha) \text{ for } \sin(\beta - \alpha) > 0 \text{ and } \cos(\beta - \alpha) > 0, \\
y_h^{fi} &= 1 - \epsilon, & y_h^V &\simeq -1 + 0.5 \cos^2(\beta - \alpha) \text{ for } \sin(\beta - \alpha) < 0 \text{ and } \cos(\beta - \alpha) > 0.
\end{aligned} \tag{5}$$

Where $|\epsilon|$ and $|\cos(\beta - \alpha)|$ are much smaller than 1. From Eq. (4), we can obtain

$$\begin{aligned}
\kappa_f &= \frac{-2 + \epsilon + 0.5 \cos(\beta - \alpha)^2}{\cos(\beta - \alpha)} < -1 \text{ for } \sin(\beta - \alpha) > 0 \text{ and } \cos(\beta - \alpha) > 0, \\
\kappa_f &= \frac{2 - \epsilon - 0.5 \cos(\beta - \alpha)^2}{\cos(\beta - \alpha)} >> 1 \text{ for } \sin(\beta - \alpha) < 0 \text{ and } \cos(\beta - \alpha) > 0.
\end{aligned} \tag{6}$$

For the type-II 2HDM, the constraints of B -meson observables and R_b generally favor $\tan\beta$ to be larger than 1, namely $\kappa_d < -1$, $\kappa_\ell < -1$, and $0 < \kappa_u < 1$ (see Eq. (4)). Therefore, according to Eq. (6), the wrong sign Yukawa coupling for the up-type quarks is generally disfavored in the type-II 2HDM. There may be the wrong sign Yukawa couplings of the down-type quark and lepton only for $\sin(\beta - \alpha) > 0$ and $\cos(\beta - \alpha) > 0$.

B. A scalar dark matter

Now we introduce the renormalizable Lagrangian of the real single scalar S ,

$$\mathcal{L}_S = -\frac{1}{2}S^2(\kappa_1\Phi_1^\dagger\Phi_1 + \kappa_2\Phi_2^\dagger\Phi_2) - \frac{m_0^2}{2}S^2 - \frac{\lambda_S}{4!}S^4. \tag{7}$$

The linear and cubic terms of the S field are forbidden by a Z'_2 symmetry $S \rightarrow -S$. The DM mass and the cubic interactions with the neutral Higgses are obtained from the Eq. (7),

$$\begin{aligned} m_S^2 &= m_0^2 + \frac{1}{2}\kappa_1 v^2 \cos^2 \beta + \frac{1}{2}\kappa_2 v^2 \sin^2 \beta, \\ -\lambda_h v S^2 h/2 &\equiv -(-\kappa_1 \sin \alpha \cos \beta + \kappa_2 \cos \alpha \sin \beta) v S^2 h/2, \\ -\lambda_H v S^2 H/2 &\equiv -(\kappa_1 \cos \alpha \cos \beta + \kappa_2 \sin \alpha \sin \beta) v S^2 H/2. \end{aligned} \quad (8)$$

III. NUMERICAL CALCULATIONS

In our discussions we take the light CP-even Higgs boson h as the SM-like Higgs, $m_h = 125$ GeV. Here we focus on examining the wrong sign Yukawa coupling of the 125 GeV Higgs in light of DM and Higgs data. Therefore, we take $\lambda_H = 0$, and the h field is the only portal between DM and SM sectors. The measurement of the branching fraction of $b \rightarrow s\gamma$ imposed a strong lower limit on the charged Higgs mass of type-II 2HDM, $m_{H^\pm} > 570$ GeV [34]. The LHC searches for the charged scalar fail to constrain the model for $m_{H^\pm} > 500$ GeV [35]. Our previous paper shows that the S , T and U oblique parameters give the strong constraints on the mass spectrum of Higgses [36]. One of m_A and m_H is around 600 GeV, another is allowed to have a wide mass range including low mass. Thus, we take $m_H = 600$ GeV and $m_A > 20$ GeV. For such case, the $SS \rightarrow AA$ annihilation channel is easy to kinematically open, and gives an important contribution to the DM relic density. If the $SS \rightarrow AA$ annihilation channel is fully responsible for the current relic density, the averaged cross section of the annihilation at present time can suffer from constraints from the Fermi-LAT search for DM annihilation from dSphs. In order to avoid the tension, we take S to be lighter than A .

In our calculation, we consider the following observables and constraints:

- (1) Theoretical constraints. In the model, the scalar potentials include the original potential type-II 2HDM and the potential of DM sector. The parameters suffer from the constraints of the vacuum stability, perturbativity, and tree-level unitarity, which are discussed in detail in Refs. [25, 27]. Here we follow the formulas in [25, 27] to perform the theoretical constraints. Note that there are additional factor of $\frac{1}{2}$ in κ_1 term and κ_2 term of this paper compared to Refs. [25, 27].

- (2) Oblique parameters. The S , T , U parameters can give stringent constraints on the mass spectrum of Higgses of 2HDM. The 2HDMC [37, 38] is used to consider the constraints from the oblique parameters (S , T , U).
- (3) The flavor observables and R_b . We include the constraints of B -meson decays from $B \rightarrow X_s \gamma$, Δm_{B_s} and Δm_{B_d} . SuperIso-3.4 [39] is employed to calculate $B \rightarrow X_s \gamma$, and Δm_{B_s} and Δm_{B_d} are calculated following the formulas in [40]. Besides, we implement the constraints of bottom quarks produced in Z decays, R_b , which is calculated using the formulas in [41, 42].
- (4) The global fit to the signal data of the 125 GeV Higgs. In this model, the 125 GeV Higgs couplings with the SM particles can be modified compared to the SM, which can give the corrections to the SM-like decay modes. In addition, if kinematically allowed, $h \rightarrow AA$ and $h \rightarrow SS$ modes can open, and enhance the total width of h sizably, which will be strongly constrained by the 125 GeV Higgs data. We perform the χ^2 calculation for the signal strengths of the 125 GeV Higgs in the $\mu_{ggF+ttH}(Y)$ and $\mu_{VBF+VH}(Y)$ with Y denoting the decay mode $\gamma\gamma$, ZZ , WW , $\tau^+\tau^-$ and $b\bar{b}$,

$$\chi^2(Y) = \begin{pmatrix} \mu_{ggH+ttH}(Y) - \hat{\mu}_{ggH+ttH}(Y) \\ \mu_{VBF+VH}(Y) - \hat{\mu}_{VBF+VH}(Y) \end{pmatrix}^T \begin{pmatrix} a_Y & b_Y \\ b_Y & c_Y \end{pmatrix} \times \begin{pmatrix} \mu_{ggH+ttH}(Y) - \hat{\mu}_{ggH+ttH}(Y) \\ \mu_{VBF+VH}(Y) - \hat{\mu}_{VBF+VH}(Y) \end{pmatrix}. \quad (9)$$

$\hat{\mu}_{ggH+ttH}(Y)$ and $\hat{\mu}_{VBF+VH}(Y)$ are the data best-fit values and a_Y , b_Y and c_Y are the parameters of the ellipse. These parameters are given by the combined ATLAS and CMS experiments [43]. We pay particular attention to the surviving samples with $\chi^2 - \chi_{\min}^2 \leq 6.18$, where χ_{\min}^2 denotes the minimum of χ^2 . These samples correspond to be within the 2σ range in any two-dimension plane of the model parameters when explaining the Higgs data.

In addition, the ATLAS and CMS reported the upper limits on the branching ratio of invisible decay of the 125 GeV Higgs. In our calculation we impose the constraints, $\text{Br}(h \rightarrow SS) < 0.16$ [43].

- (5) The non-observation of additional Higgs bosons. The HiggsBounds [44, 45] is used

Channel	Experiment	Mass range (GeV)	Luminosity
$gg/b\bar{b} \rightarrow A/H \rightarrow \tau^+\tau^-$	ATLAS 8 TeV [47]	90-1000	19.5-20.3 fb ⁻¹
$gg/b\bar{b} \rightarrow A/H \rightarrow \tau^+\tau^-$	CMS 8 TeV [48]	90-1000	19.7 fb ⁻¹
$b\bar{b} \rightarrow A/H \rightarrow \tau^+\tau^-$	CMS 8 TeV [49]	25-80	19.7 fb ⁻¹
$gg/b\bar{b} \rightarrow A/H \rightarrow \tau^+\tau^-$	ATLAS 13 TeV [50]	200-1200	13.3 fb ⁻¹
$gg/b\bar{b} \rightarrow A/H \rightarrow \tau^+\tau^-$	CMS 13 TeV [51]	90-3200	12.9 fb ⁻¹
$gg \rightarrow h \rightarrow AA \rightarrow \tau^+\tau^-\tau^+\tau^-$	ATLAS 8 TeV [52]	4-50	20.3 fb ⁻¹
$pp \rightarrow h \rightarrow AA \rightarrow \tau^+\tau^-\tau^+\tau^-$	CMS 8 TeV [53]	5-15	19.7 fb ⁻¹
$pp \rightarrow h \rightarrow AA \rightarrow (\mu^+\mu^-)(b\bar{b})$	CMS 8 TeV [53]	25-62.5	19.7 fb ⁻¹
$pp \rightarrow h \rightarrow AA \rightarrow (\mu^+\mu^-)(\tau^+\tau^-)$	CMS 8 TeV [53]	15-62.5	19.7 fb ⁻¹
$gg \rightarrow A \rightarrow hZ \rightarrow (\tau^+\tau^-)(\ell\ell)$	CMS 8 TeV [54]	220-350	19.7 fb ⁻¹
$gg \rightarrow A \rightarrow hZ \rightarrow (b\bar{b})(\ell\ell)$	CMS 8 TeV [55]	225-600	19.7 fb ⁻¹
$gg \rightarrow A \rightarrow hZ \rightarrow (\tau^+\tau^-)Z$	ATLAS 8 TeV [56]	220-1000	20.3 fb ⁻¹
$gg \rightarrow A \rightarrow hZ \rightarrow (b\bar{b})Z$	ATLAS 8 TeV [56]	220-1000	20.3 fb ⁻¹
$gg/b\bar{b} \rightarrow A \rightarrow hZ \rightarrow (b\bar{b})Z$	ATLAS 13 TeV [57]	200-2000	3.2 fb ⁻¹

TABLE I: The upper limits at 95% C.L. on the production cross-section times branching ratio of the processes considered in the H and A searches at the LHC.

to implement the exclusion constraints from the searches for the neutral and charged Higgs at LEP at 95% confidence level.

At the LHC the ATLAS and CMS have searched for additional scalar state via its decay into various SM channels and some exotic decays. There are destructive interference contributions of b -quark loop and top quark loop for $gg \rightarrow A$ production in type-II 2HDM. The cross section decreases with increasing of $\tan\beta$, reaches the minimum value for the moderate value of $\tan\beta$, and is dominated by the b -quark loop for enough large value of $\tan\beta$. For $gg \rightarrow H$ production, the cross section depends on $\sin(\beta-\alpha)$ in addition to $\tan\beta$ and m_H . We employ **SusHi** [46] to compute cross sections for H and A in the gluon fusion and $b\bar{b}$ -associated production at NNLO in QCD. A complete list of the searches for additional Higgs considered by us is summarized in Table I where some channels are taken from ref. [58]. Our previous paper shows that $\tan\beta$ is nearly required to be larger than 3.0 in the case of the wrong sign Yukawa coupling of the 125

GeV Higgs [36]. For such large $\tan\beta$, $\sigma(gg \rightarrow A)$, $\text{Br}(A \rightarrow \gamma\gamma)$ and $\sigma(gg \rightarrow H)$ are sizably suppressed. Therefore, the $A \rightarrow \gamma\gamma$ channels fail to constrain the parameter space. In addition, considering that m_H is fixed at a large value, $m_H = 600$ GeV, the $H \rightarrow \gamma\gamma$, WW , ZZ , hh , AZ channels can be safely ignored. In fact, in our previous paper [36], we included these channels, and found that these channels can not impose constraints on the parameter space in the case of the wrong sign Yukawa coupling and $m_H = 600$ GeV.

- (6) The observables of DM. We employ `micrOMEGAs` [59] to calculate the relic density and the today DM pair-annihilation cross sections. The model file is generated by `FeynRules` [60].

For a small m_S , the $SS \rightarrow gg, c\bar{c}, \tau^+\tau^-, b\bar{b}$ annihilation channels play the important contributions to the DM relic density. With increasing of m_S , the contributions of $SS \rightarrow WW, ZZ, hh, t\bar{t}$ become important. In addition to annihilation to the SM particles, the DM can annihilate to $AA, HH, H^\pm H^\mp$, and hH if kinematically allowed. In this model, the elastic scattering of S on a nucleon receives the contributions from the h exchange diagrams. The spin-independent cross section is written as [61],

$$\sigma_{p(n)} = \frac{\mu_{p(n)}^2}{\pi m_S^2} [f^{p(n)}]^2, \quad (10)$$

where $\mu_{p(n)} = \frac{m_S m_{p(n)}}{m_S + m_{p(n)}}$,

$$f^{p(n)} = \sum_{q=u,d,s} f_q^{p(n)} \mathcal{C}_{Sq} \frac{m_{p(n)}}{m_q} + \frac{2}{27} f_g^{p(n)} \sum_{q=c,b,t} \mathcal{C}_{Sq} \frac{m_{p(n)}}{m_q}, \quad (11)$$

with $\mathcal{C}_{Sq} = \frac{\lambda_h m_q}{m_h^2} y_q$. Following the recent study [62], we take

$$\begin{aligned} f_u^{(p)} &\approx 0.0208, & f_d^{(p)} &\approx 0.0399, & f_s^{(p)} &\approx 0.0430, & f_g^{(p)} &\approx 0.8963, \\ f_u^{(n)} &\approx 0.0188, & f_d^{(n)} &\approx 0.0440, & f_s^{(n)} &\approx 0.0430, & f_g^{(n)} &\approx 0.8942. \end{aligned} \quad (12)$$

If $f_q^{(p)} = f_q^{(n)}$ and $f_g^{(p)} = f_g^{(n)}$ are satisfied, the S -nucleon coupling is always isospin-conserved. If the relations are not satisfied, the S -nucleon coupling may be violated for the appropriate values of y_d and y_u .

Recently, the density of cold DM in the universe was estimated by the Planck collaboration to be $\Omega_c h^2 = 0.1198 \pm 0.0015$ [63]. The strongest constraints on the spin-independent DM-nucleon cross section are from the PandaX-II (2017) for a DM with

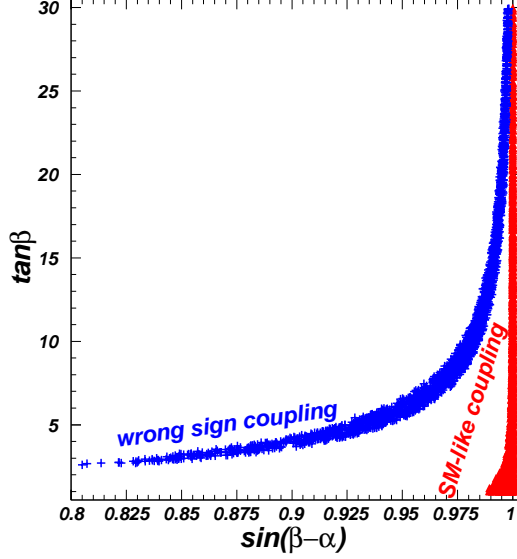


FIG. 1: The samples surviving from the constraints of the 125 GeV Higgs signal data projected on the plane of $\sin(\beta - \alpha)$ versus $\tan \beta$.

mass larger than 100 GeV [31], and from the XENON1T (2017) for a DM with mass smaller than 60 GeV [30]. For a DM with mass in the range of 60 GeV and 100 GeV, the upper limits of PandaX-II (2017) are nearly the same as those of XENON1T (2017). The Fermi-LAT search for the DM annihilation from dSphs gave the upper limits on the averaged cross sections of the DM annihilation to e^+e^- , $\mu^+\mu^-$, $\tau^+\tau^-$, $u\bar{u}$, $b\bar{b}$, and WW [32].

IV. RESULTS AND DISCUSSIONS

In Fig. 1, we show $\sin(\beta - \alpha)$ and $\tan \beta$ allowed by the signal data of the 125 GeV Higgs. Fig. 1 shows that $\sin(\beta - \alpha)$ is required to be very close to 1 in the case of the SM-like Higgs coupling of the 125 GeV Higgs, $\sin(\beta - \alpha) > 0.99$. However, in the case of the wrong sign Yukawa coupling of the 125 GeV Higgs, $\sin(\beta - \alpha)$ is allowed to be much smaller than 1, and $\tan \beta$ is restricted to a very narrow range for a given value of $\sin(\beta - \alpha)$, such as $5.4 < \tan \beta < 6.6$ for $\sin(\beta - \alpha) = 0.95$. The surviving samples with the wrong sign Yukawa coupling are projected on the planes of y_d/y_u versus $\tan \beta$ and y_d/y_u versus $\sin(\beta - \alpha)$ in Fig. 2. As discussed above, the down-type quark Yukawa coupling of the 125 GeV Higgs has an opposite sign to the Yukawa coupling of up-type quark. y_d/y_u is allowed to vary from -1.2 to -0.65, and the absolute value increases with $\tan \beta$ and $\sin(\beta - \alpha)$.

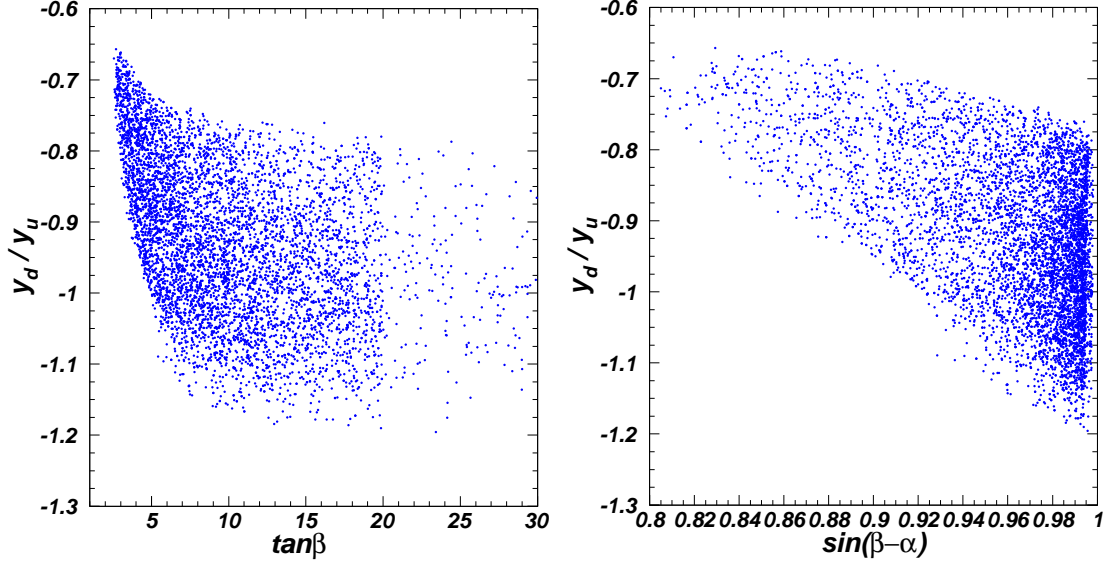


FIG. 2: In the case of the wrong sign Yukawa coupling of the 125 GeV Higgs, the samples surviving from the constraints of the 125 GeV Higgs signal data projected on the planes of y_d/y_u versus $\tan \beta$ and y_d/y_u versus $\sin(\beta - \alpha)$. y_d (y_u) denotes the normalized factor of down-type (up-type) quark Yukawa coupling of the 125 GeV Higgs with respect to the SM.

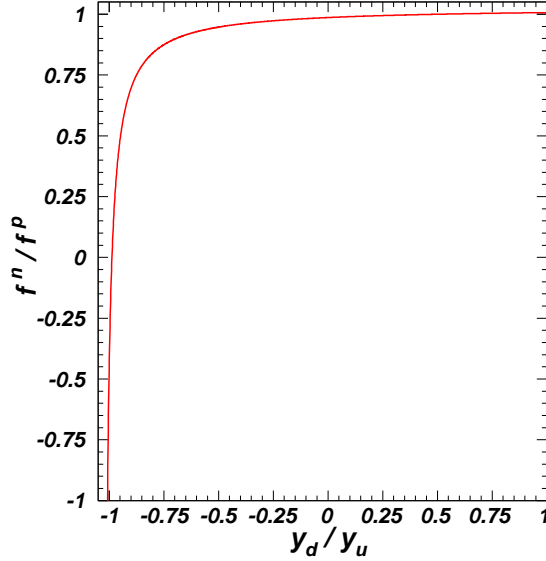


FIG. 3: f^n/f^p versus y_d/y_u .

In Fig. 3, we show f^n/f^p versus y_d/y_u . Since the hadronic quantities in the spin-independent DM-nucleon scattering are fixed, f^n/f^p only depends on the normalized factors of Yukawa couplings, y_u and y_d . The f^n/f^p is very sensitive to y_d/y_u when y_d/y_u is around -1.0, and very close to 1.0 for $y_d/y_u > 0$. In the following discussions, we will focus on the surviving samples with $-1.0 < f^n/f^p < 1.0$ where the upper limits on the spin-independent

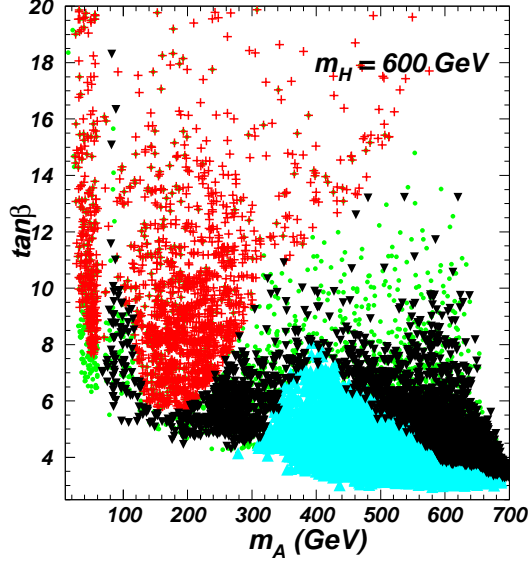


FIG. 4: In the wrong sign Yukawa coupling of the 125 GeV Higgs, the surviving samples projected on the plane of $\tan\beta$ versus m_A . All the samples are allowed by the constraints of "pre-LHC" and the 125 GeV Higgs signal data. Also the constraints of the DM relic density and the searches for Higgs at LHC are satisfied for the inverted triangles (black). The pluses (red) and triangles (sky blue) are respectively excluded by the $A/H \rightarrow \tau^+\tau^-$ and $A \rightarrow hZ$ searches at LHC.

DM-nucleon cross section from the XENON1T (2017) and PandaX-II (2017) can be weakened.

In Fig. 4, we project the surviving samples on the planes of $\tan\beta$ versus m_A after imposing the constraints of "pre-LHC" (denoting the theory, the oblique parameters, the flavor observables, R_b , and the exclusion limits from searches for Higgs at LEP), the signal data of the 125 GeV Higgs, the searches for the additional Higgs at LHC, and the DM relic density. Since the signal data of the 125 GeV Higgs impose very strong constraints on the width of ($h \rightarrow AA$), the $h \rightarrow AA$ channels at the LHC fail to give the constraints on the parameter space. The AhZ coupling is proportional to $\cos(\beta - \alpha)$, and $\sin(\beta - \alpha)$ increases with $\tan\beta$. Therefore, the $A \rightarrow hZ$ channel can impose a lower bound on $\tan\beta$ for $m_A > 280$ GeV. While the $b\bar{b} \rightarrow A \rightarrow \tau^+\tau^-$ channel can impose an upper bound on $\tan\beta$. For $140 \text{ GeV} < m_A < 200 \text{ GeV}$, $\tan\beta$ is restricted to a very narrow range, $4.2 < \tan\beta < 5.7$. However, for m_A around 80 GeV, $\tan\beta$ is allowed to be as large as 18. The correct DM relic density can be obtained for the nearly whole parameter space of m_A and $\tan\beta$. Certainly the relic density is sensitive to the DM mass and the DM coupling with the 125 GeV Higgs.

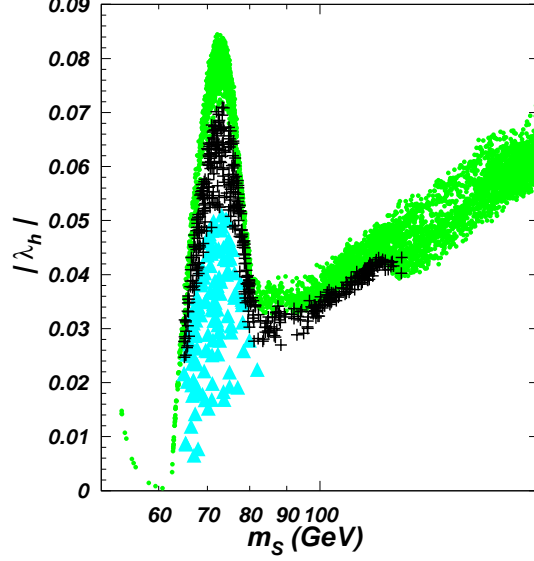


FIG. 5: The surviving samples projected on the plane of $|\lambda_h|$ versus m_S . All the samples are allowed by the constraints of "pre- $\Omega_c h^2$ " and the DM relic density. The contribution of $SS \rightarrow AA$ to $1/(\Omega h^2)$ is 0 ~ 10% for the bullets (green), 10% ~ 50% for the pluses (black), and 50% ~ 100% for triangles (sky blue).

In Fig. 5, we project the surviving samples on the plane of $|\lambda_h|$ versus m_S after imposing the constraints of the DM relic density and "pre- $\Omega_c h^2$ " (denoting "pre-LHC", the 125 GeV Higgs signal data, and the searches for Higgs at LHC). From Fig. 5 we find the $SS \rightarrow AA$ annihilation channel can play an important contribution to the DM relic density, especially for $65 \text{ GeV} < m_S < 85 \text{ GeV}$. In such range, the DM mass deviates from the resonance region, and the $SS \rightarrow WW^{(*)}$ channel is kinematically suppressed. Therefore, the contribution of $SS \rightarrow AA$ to the relic density can be dominant. Due to the contribution of $SS \rightarrow AA$ channel to the relic density, the DM coupling with the 125 GeV Higgs can be sizably suppressed. For example, when the contribution of $SS \rightarrow AA$ to $1/(\Omega h^2)$ is smaller than 10%, $|\lambda_h|$ is required to be in the range of 0.065 and 0.08 for $m_S = 70 \text{ GeV}$. When the contribution of $SS \rightarrow AA$ is dominant, $|\lambda_h|$ is allowed to be as low as 0.015 for $m_S = 70 \text{ GeV}$. However, for $m_S < 60 \text{ GeV}$, the $SS \rightarrow AA$ annihilation channel can not give sizable contribution to the relic density. For such case, the $h \rightarrow AA$ decay mode will open, and enhance the total width of the 125 GeV Higgs. The signal data of the 125 GeV Higgs will give the strong constraints on the hAA coupling in addition to the hSS coupling. Due to the tension between the DM relic density and the signal data of the 125 GeV Higgs, $m_S < 50$

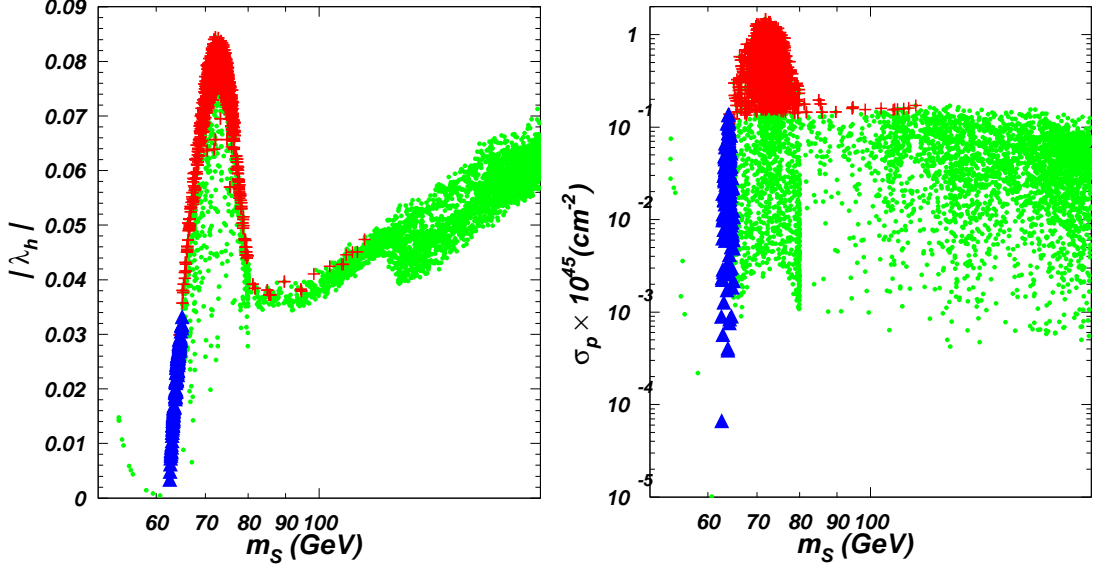


FIG. 6: The surviving samples projected on the planes of $|\lambda_h|$ versus m_S and σ_p versus m_S . All the samples are allowed by the constraints of "pre- $\Omega_c h^2$ " and the DM relic density. The pluses (red) are excluded by the constraints on the spin-independent DM-proton cross section from XENON1T (2017) and PandaX-II (2017). The triangles (royal blue) are excluded by the Fermi-LAT search for DM annihilation from dSphs.

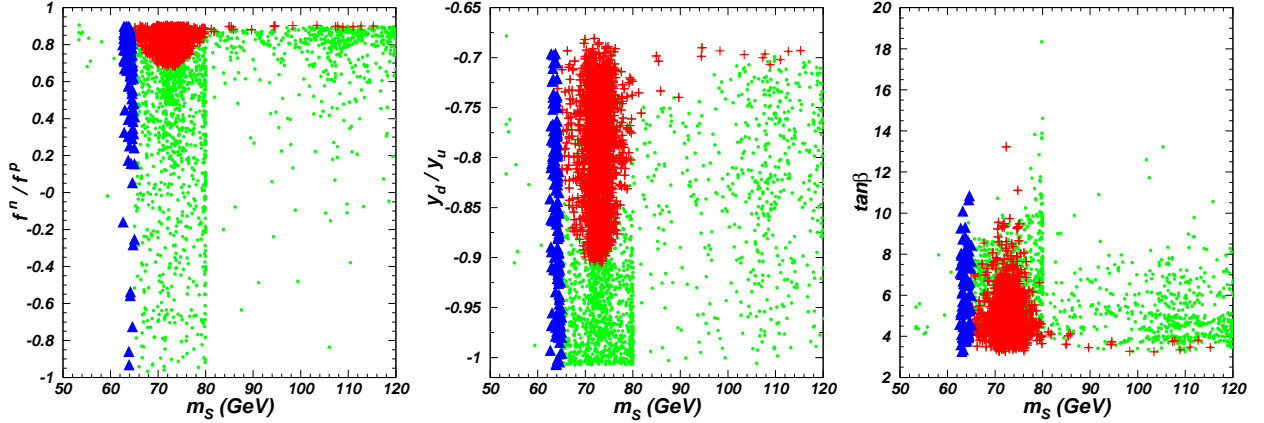


FIG. 7: Same as Fig. 6, but projected on the planes of f^n/f^p versus m_S , y_d/y_u versus m_S , and $\tan \beta$ versus m_S .

GeV is excluded. Besides, a very small $|\lambda_h|$ still can achieve the correct relic abundance at the resonance, m_S around 60 GeV.

In Fig. 6 and Fig. 7, we project the surviving samples on the planes of $|\lambda_h|$, σ_p , f^n/f^p , y_d/y_u , and $\tan \beta$ versus m_S after imposing the constraints of "pre- $\Omega_c h^2$ ", the DM relic density, XENON1T (2017), PandaX-II (2017), and the Fermi-LAT search for DM

annihilation from dSphs. The right panel of Fig. 6 shows that the upper limits of XENON1T (2017) and PandaX-II (2017) exclude the samples with $\sigma_p > 10^{-46} \text{ cm}^{-2}$ and $64 \text{ GeV} < m_S < 116 \text{ GeV}$. The left panel of Fig. 6 shows that for $64 \text{ GeV} < m_S < 80 \text{ GeV}$, the relic density allows $|\lambda_h|$ to have a relatively large value, which can lead the spin-independent σ_p to be much larger than the upper limits of XENON1T (2017) and PandaX-II (2017). In the range of $64 \text{ GeV} < m_S < 80 \text{ GeV}$, there are also many samples surviving from the constraints of XENON1T (2017) and PandaX-II (2017), especially for the case that $SS \rightarrow AA$ plays an important contribution to the relic density. For such case, λ_h can be sizably suppressed, leading σ_p to accommodate the upper limits of XENON1T (2017) and PandaX-II (2017). The Fermi-LAT limits can exclude most of samples in the range of $62.5 \text{ GeV} < m_S < 65 \text{ GeV}$, even including the sample with $\sigma_p \sim 6 \times 10^{-50} \text{ cm}^{-2}$ and $m_S \sim 62.5 \text{ GeV}$. For such sample, the DM pair-annihilation can be sizably enhanced at the resonance, but the spin-independent DM-nucleon cross section has no resonance enhancement. When m_S is moderately smaller than $m_h/2$, a very small $|\lambda_h|$ can achieve the correct relic abundance since the integral in the calculation of thermal average can be dominated by the resonance at $s = m_h^2$ with s being the squared center-of-mass energy of the pair-annihilation of DM. For such case, the today averaged cross section of DM pair-annihilation can be sizably suppressed since the velocity of DM at the present time is much smaller than that in the early universe. Therefore, the limits of Fermi-LAT search for DM annihilation from dSphs can be satisfied when m_S is moderately smaller than $m_h/2$.

Fig. 7 shows that the constraints of XENON1T (2017) and PandaX-II (2017) exclude most of samples in the ranges of $64 \text{ GeV} < m_S < 80 \text{ GeV}$, $0.65 < f^n/f^p < 1$, and $y_d/y_u > -0.91$. In the ranges of $80 \text{ GeV} < m_S < 116 \text{ GeV}$, $-1 < f^n/f^p < 0.85$, $y_d/y_u < -0.75$, and $\tan\beta > 4.5$, the upper limits of XENON1T (2017) and PandaX-II (2017) can be satisfied. The DM scattering rate with Xe target can be sizably suppressed for f^n/f^p around -0.7, thus weakening the constraints from XENON1T (2017) and PandaX-II. However, for f^n/f^p around -0.7, the Fermi-LAT still can exclude the samples in the range of $62.5 \text{ GeV} < m_S < 65 \text{ GeV}$.

V. CONCLUSION

The wrong sign Yukawa coupling of the 125 GeV Higgs is an interesting characteristic of 2HDM. Such a scalar is taken as the portal between DM and SM sectors, the large isospin-violating coupling of DM-nucleon can be realized. We examine the wrong sign Yukawa coupling of the 125 GeV Higgs which is the only portal between DM and SM sectors in the framework of the type-II 2HDM with a scalar DM. After imposing the constraints from the theory, oblique parameters, the flavor observables, the Higgs searches at the LHC, and the DM experiments, we obtain some interesting observables:

(i) In the case of the wrong sign Yukawa coupling of the 125 GeV Higgs, the searches for additional Higgs via $\tau^+\tau^-$ channel at the LHC can impose an upper limit on $\tan\beta$, and the $A \rightarrow hZ$ channel can impose a lower limit on $\tan\beta$.

(ii) The $SS \rightarrow AA$ annihilation channel can play an important contribution to the DM relic density, especially for $65 \text{ GeV} < m_S < 85 \text{ GeV}$. Due to the tension between the DM relic density and the signal data of the 125 GeV Higgs, $m_S < 50 \text{ GeV}$ is excluded.

(iii) The upper limits of XENON1T (2017) and PandaX-II (2017) on the spin-independent DM-nucleon cross section exclude most of samples in the ranges of $64 \text{ GeV} < m_S < 80 \text{ GeV}$, $0.65 < f^n/f^p < 1$, and $y_d/y_u > -0.91$. For $80 \text{ GeV} < m_S < 116 \text{ GeV}$, some samples with $y_d/y_u > -0.75$ are excluded by the constraints of XENON1T (2017) and PandaX-II (2017).

(iv) The Fermi-LAT limits can exclude most of samples in the range of $62.5 \text{ GeV} < m_S < 65 \text{ GeV}$. For m_S around $m_h/2$, the sample with $f^n/f^p \sim -0.7$ can still be excluded by the Fermi-LAT limits.

Acknowledgment

We thank Prof. Junjie Cao for helpful discussions. This work is supported by the National Natural Science Foundation of China under grant No. 11575152.

-
- [1] T. D. Lee, Phys. Rev. D **8**, 1226 (1973).
 - [2] H. E. Haber, G. L. Kane and T. Sterling, Nucl. Phys. B **161**, 493 (1979).
 - [3] L. J. Hall and M. B. Wise, Nucl. Phys. B **187**, 397 (1981).

- [4] J. F. Donoghue and L. F. Li, Phys. Rev. D **19**, 945 (1979).
- [5] V. D. Barger, J. L. Hewett and R. J. N. Phillips, Phys. Rev. D **41**, 3421 (1990).
- [6] Y. Grossman, Nucl. Phys. B **426**, 3 (1994).
- [7] A. G. Akeroyd and W. J. Stirling, Nucl. Phys. B **447**, 3 (1995).
- [8] A. G. Akeroyd, Phys. Lett. B **377**, 95 (1996).
- [9] I. F. Ginzburg, M. Krawczyk, P. Osland, arXiv:hep-ph/0101208.
- [10] P. M. Ferreira, J. F. Gunion, H. E. Haber and R. Santos, Phys. Rev. D **89**, 115003 (2014).
- [11] B. Dumont, J. F. Gunion, Y. Jiang and S. Kraml, Phys. Rev. D **90**, 035021 (2014).
- [12] D. Fontes, J. C. Romo and J. P. Silva, Phys. Rev. D **90**, 015021 (2014).
- [13] P. M. Ferreira, J. F. Gunion, H. E. Haber, R. Santos, Phys. Rev. D **89**, 115003 (2014).
- [14] D. Fontes, J. C. Romao, J. P. Silva, Phys. Rev. D **90**, 015021 (2014).
- [15] P. M. Ferreira, R. Guedes, M. O. P. Sampaio, R. Santos, JHEP **1412**, 067 (2014).
- [16] L. Wang, X.-F. Han, JHEP **1411**, 085 (2014).
- [17] A. Biswas, A. Lahiri, Phys. Rev. D **93**, 115017 (2016).
- [18] T. Modak, J. C. Romao, S. Sadhukhan, J. P. Silva, R. Srivastava, Phys. Rev. D **94**, 075017 (2016).
- [19] D. Das, A. Kundu, I. Saha, arXiv:1707.03000.
- [20] L. Wang, X.-F. Han, JHEP **1505**, 039 (2015).
- [21] T. Abe, R. Sato, K. Yagyu, JHEP **1507**, 064 (2015).
- [22] X.-G. He, J. Tandean, Phys. Rev. D **88**, 013020 (2013).
- [23] Y. Cai, T. Li, Phys. Rev. D **88**, 115004 (2013).
- [24] L. Wang, X.-F. Han, Phys. Lett. B **739**, 416-420 (2014).
- [25] A. Drozd, B. Grzadkowski, J. F. Gunion, Y. Jiang, JHEP **1411**, 105 (2014).
- [26] A. Drozd, B. Grzadkowski, J. F. Gunion, Y. Jiang, JCAP **1610**, 040 (2016).
- [27] X.-G. He, J. Tandean, JHEP **1612**, 074 (2016).
- [28] T. Alanne, K. Kainulainen, K. Tuominen, V. Vaskonen, JCAP **1608**, 057 (2016).
- [29] D. S. Akerib et al. (LUX Collaboration), Phys. Rev. Lett. **118**, 021303 (2017).
- [30] E. Aprile et al. [XENON Collaboration], arXiv:1705.06655.
- [31] PandaX Collaboration, arXiv:1708.06917.
- [32] Fermi-LAT Collaboration, Phys. Rev. Lett. **115**, 231301 (2015).
- [33] R. A. Battye, G. D. Brawn, A. Pilaftsis, JHEP **1108**, 020 (2011).

- [34] Heavy Flavor Averaging Group, arXiv:1612.07233; M. Misiak, M. Steinhauser, Eur. Phys. Jour. C **77**, 201 (2017).
- [35] S. Moretti, arXiv:1612.02063.
- [36] L. Wang, F. Zhang, X.-F. Han, Phys. Rev. D **95**, 115014 (2017).
- [37] D. Eriksson, J. Rathsman, O. Stål, Comput. Phys. Commun. **181**, 189 (2010).
- [38] D. Eriksson, J. Rathsman, O. Stål, Comput. Phys. Commun. **181**, 833 (2010).
- [39] F. Mahmoudi, Comput. Phys. Commun. **180**, 1579-1673 (2009).
- [40] C. Q. Geng and J. N. Ng, Phys. Rev. D **38**, 2857 (1988) [Erratum-ibid. D 41, 1715 (1990)].
- [41] H. E. Haber, H. E. Logan, Phys. Rev. D **62**, 015011 (2010).
- [42] G. Degrand, P. Slavich, Phys. Rev. D **81**, 075001 (2010).
- [43] ATLAS and CMS Collaborations, JHEP **1608**, (2016) 045.
- [44] P. Bechtle, O. Brein, S. Heinemeyer, G. Weiglein, K. E. Williams, Comput. Phys. Commun. **181**, 138-167 (2010).
- [45] P. Bechtle, O. Brein, S. Heinemeyer, O. Stål, T. Stefaniak, G. Weiglein, K. E. Williams, Eur. Phys. Jour. C **74**, 2693 (2014).
- [46] R. V. Harlander, S. Liebler and H. Mantler, Comput. Phys. Commun. **184**, 1605 (2013).
- [47] ATLAS Collaboration, G. Aad *et al.*, “Search for neutral Higgs bosons of the minimal supersymmetric standard model in pp collisions at $\sqrt{s} = 8$ TeV with the ATLAS detector,” JHEP **11**, 056 (2014).
- [48] CMS Collaboration, “Search for additional neutral Higgs bosons decaying to a pair of tau leptons in pp collisions at $\sqrt{s} = 7$ and 8 TeV,” CMS-PAS-HIG-14-029.
- [49] CMS Collaboration, “Search for a low-mass pseudoscalar Higgs boson produced in association with a $b\bar{b}$ pair in pp collisions at $\sqrt{s} = 8$ TeV,” arXiv:1511.03610.
- [50] ATLAS Collaboration, “Search for Minimal Supersymmetric Standard Model Higgs Bosons H/A in the $\tau\tau$ final state in up to 13.3 fb⁻¹ of pp collisions at $\sqrt{s} = 13$ TeV with the ATLAS Detector,” ATLAS-CONF-2016-085.
- [51] CMS Collaboration, “Search for a neutral MSSM Higgs Boson decaying into $\tau\tau$ H/A with 12.9 fb⁻¹ of data at $\sqrt{s} = 13$ TeV,” CMS-PAS-HIG-16-037.
- [52] ATLAS Collaboration, “Search for Higgs bosons decaying to aa in the $\mu\mu\tau\tau$ final state in pp collisions at $\sqrt{s} = 8$ TeV with the ATLAS experiment,” Phys. Rev. D **92**, 052002 (2015).
- [53] CMS Collaboration, “Search for light bosons in decays of the 125 GeV Higgs boson in proton-

- proton collisions at $\sqrt{s}=8$ TeV,” arXiv:1701.02032 .
- [54] CMS Collaboration, V. Khachatryan *et al.*, “Searches for a heavy scalar boson H decaying to a pair of 125 GeV Higgs bosons hh or for a heavy pseudoscalar boson A decaying to Zh, in the final states with $h \rightarrow \tau\tau$,” Phys. Lett. B **755**, 217-244 (2016).
 - [55] CMS Collaboration, V. Khachatryan *et al.*, “Search for a pseudoscalar boson decaying into a Z boson and the 125 GeV Higgs boson in $\ell^+\ell^-b\bar{b}$ final states,” Phys. Lett. B **748**, 221-243 (2015).
 - [56] ATLAS Collaboration, G. Aad *et al.*, “Search for a CP-odd Higgs boson decaying to Zh in pp collisions at $\sqrt{s}=8$ TeV with the ATLAS detector,” Phys. Lett. B **744**, 163-183 (2015).
 - [57] ATLAS Collaboration, “Search for a CP-odd Higgs boson decaying to Zh in pp collisions at $\sqrt{s}=13$ TeV with the ATLAS detector,” ATLAS-CONF-2016-015.
 - [58] R. K. Barman, B. Bhattacharjee, A. Choudhury, D. Chowdhury, J. Lahiri, S. Ray, arXiv:1608.02573.
 - [59] G. Belanger, F. Boudjema, A. Pukhov, A. Semenov, Comput. Phys. Commun. **185**, 960-985 (2014).
 - [60] A. Alloul et al., Comput. Phys. Commun. **185**, 2250 (2014).
 - [61] G. Jungman, M. Kamionkowski, K. Griest, Phys. Rept. **267**, 195 (1996); M. A. Shifman, A. I. Vainshtein and V. I. Zakharov, Phys. Lett. B **78**, 443 (1978).
 - [62] A. Crivellin, M. Hoferichter, M. Procura, Phys. Rev. D **89**, 054021 (2014).
 - [63] Planck Collaboration, Astron. Astrophys. A **27**, 594 (2016).